



JUNO: A Next Generation Reactor Antineutrino Experiment

Liang Zhan

*Institute of High Energy Physics, Chinese Academy of Sciences, Beijing 100049, China
zhanl@ihep.ac.cn*

Abstract

The mass hierarchy and the CP phase are the main focus of the next generation neutrino oscillation experiments. Jiangmen Underground Neutrino Observatory (JUNO), as a medium baseline reactor antineutrino experiment, can determine the neutrino mass hierarchy independent of the CP phase. The physics potential on the mass hierarchy, and other measurements are reviewed. The preliminary design options for a 20 kton detector with an energy resolution of $3\%/\sqrt{E_{vis}}$ are illustrated. The main technical challenges on the PMT and scintillator are discussed and the corresponding R&D efforts are presented.

Keywords: JUNO, mass hierarchy

1. Introduction

A large neutrino mixing angle θ_{13} was observed by the latest reactor [1, 2, 3, 4, 5] and accelerator [6, 7] neutrino oscillation experiments. In the next few years, the precision of $\sin^2 2\theta_{13}$ can reach to 3% by continuous running of Daya Bay. The remaining unknown parameters are the neutrino mass hierarchy (the sign of Δm_{31}^2 or Δm_{32}^2) and the CP phase, which are the focus of next generation neutrino oscillation experiments. One possibility to determine the mass hierarchy is to measure the mass effect which is different for normal hierarchy and inverted hierarchy, and hence atmospheric [8, 9] and accelerator [10, 11, 12] neutrino experiments are proposed. Another possibility is raised [13, 14, 15, 16, 17] to use the oscillation interference effect between Δm_{31}^2 and Δm_{32}^2 by reactor antineutrinos.

The Jiangmen Underground Neutrino Observatory (JUNO) uses 20 kton liquid scintillator (LS) as detector target. The primary goal is to determine the mass hierarchy using the reactor antineutrinos by precise measuring the oscillation spectrum with a $3\%/\sqrt{E_{vis}}$ energy resolution. A candidate site is located at Jiangmen in South China, with baselines around 53 km from Taishan and Jiangmen nuclear power plants, shown in Fig-

ure 1. In addition to the mass hierarchy, such a large and high precision detector has other rich physics potentials. The neutrino mixing parameters (Δm_{21}^2 , Δm_{31}^2 and $\sin^2 \theta_{12}$) can be measured with a precision better than 1%. JUNO detector is also sensitive to supernova neutrinos, geo-neutrinos, solar neutrinos and atmospheric neutrinos, and can probe the sterile neutrinos and exotic physics like nucleon decays.

2. Sensitivity to mass hierarchy

At the candidate site, the baselines and the reactor power of the nuclear power plants are listed [18] in Table 1. The Yangjiang and Taishan reactor power plants are under construction and will be completed around 2020. The site was selected to minimize the baseline difference between Yangjiang and Taishan reactor cores for better sensitivity, which will be discussed later. The survival probability of the reactor antineutrinos can be written as

$$P_{ee} = 1 - \cos^4 \theta_{13} \sin^2 2\theta_{12} \sin^2 \Delta_{21} - \cos^2 \theta_{12} \sin^2 2\theta_{13} \sin^2 \Delta_{31} - \sin^2 \theta_{12} \sin^2 2\theta_{13} \sin^2 \Delta_{32}, \quad (1)$$



Figure 1: Candidate site of the JUNO experiment.

Cores	TS-C1	TS-C2	TS-C3	TS-C4
Power (GW)	4.6	4.6	4.6	4.6
Baseline(km)	52.76	52.63	52.32	52.20
Cores	YJ-C1	YJ-C2	YJ-C3	YJ-C4
Power (GW)	2.9	2.9	2.9	2.9
Baseline(km)	52.75	52.84	52.42	52.51
Cores	YJ-C5	YJ-C6	DYB	HZ
Power (GW)	2.9	2.9	17.4	17.4
Baseline(km)	52.12	52.21	215	265

Table 1: List of the baselines and reactor power for the Yangjiang (YJ) and Taishan (TS) reactor power plants, as well as the remote reactors of Daya Bay (DYB) and Huizhou (HZ), at the candidate site.

where $\Delta_{ij} = 1.27\Delta m_{ij}^2 L/E$, Δm_{ij}^2 is neutrino mass-squared difference ($m_i^2 - m_j^2$) in eV^2 , θ_{ij} is neutrino mixing angle, L is the baseline length from reactor to $\bar{\nu}_e$ detector in meter, and E is the $\bar{\nu}_e$ energy in MeV. The reactor antineutrinos can be detected in liquid scintillator detector via coincident signals of inverse β decay (IBD), $\bar{\nu}_e + p \rightarrow e^+ + n$. More than hundred thousand IBD signals can be collected by 6 year running, assuming an 80% effective detection efficiency (considering event selection efficiency, live time ratio and reactor full power ratio).

To calculate the sensitivity of mass hierarchy, we fit the simulated spectrum to the normal hierarchy (NH) and inverted hierarchy (IH) cases respectively using a

χ^2 function,

$$\chi^2 = \sum_i \frac{(T_i - F_i(1 + \epsilon + \epsilon_i))^2}{T_i} + \sum_p \frac{(p_f - p_t)^2}{\sigma_p^2} + \sum_i \frac{\epsilon_i^2}{\sigma_i^2}, \quad (2)$$

where T_i is the input antineutrino spectrum assuming the truth is NH or IH, F_i is the fitted spectrum. The ϵ is the normalization factor of the antineutrino spectrum and it is floating in the χ^2 function. There is no constrain on ϵ and it means we only use the shape information. The ϵ_i is uncorrelated between bins and so the shape can fluctuate. The p in χ^2 function denotes the oscillation parameters, including $\sin^2 2\theta_{13}$, $\sin^2 \theta_{12}$, Δm_{21}^2 , and Δm_{ee}^2 (an effective mass-squared difference defined as a combination of Δm_{31}^2 and Δm_{32}^2 [18]). The p_f and p_t are fitted and input oscillation parameters respectively. The σ_p^2 is the uncertainty of the corresponding oscillation parameter. As expected, the spectrum can fit the input spectrum better if using the truth mass hierarchy. Assuming NH is the truth, we try two fits using NH spectrum and IH spectrum respectively and get two corresponding minimal χ^2 , namely $\chi_{\min}^2(\text{NH})$ and $\chi_{\min}^2(\text{IH})$. A discriminator can be defined as

$$\Delta\chi^2 = \chi_{\min}^2(\text{IH}) - \chi_{\min}^2(\text{NH}), \quad (3)$$

A median sensitivity [19], approximately $\sqrt{\Delta\chi^2}\sigma$, is often used when comparing the sensitivity of different experiments.

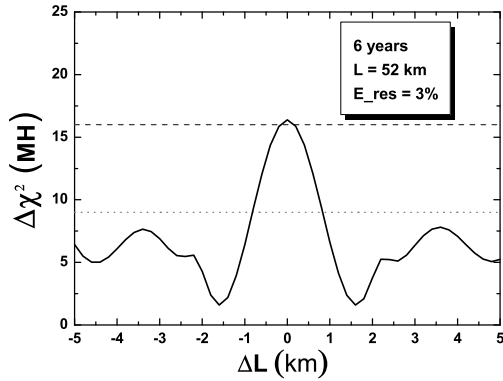


Figure 2: The variation (left panel) of the MH sensitivity as a function of the baseline difference of two reactors.

Using the nominal reactor setup list in Table 1 and a 20 kton liquid scintillator detector with a $3\%/\sqrt{E_{vis}}$ energy resolution, we get $\Delta\chi^2 \approx 11$ ($\sim 3.3\sigma$ at median sensitivity) by a 6 year running. The importance of the site selection is shown in Figure 2. Assuming two groups of reactors, the sensitivity decreases fast if the baselines are not equal. As a result, $\Delta\chi^2$ is degraded from 16 at an ideal site with equal baselines to 11 at the candidate site. We find the uncertainties of $\sin^2 2\theta_{13}$, $\sin^2 \theta_{12}$, Δm_{21}^2 have slight impacts to the sensitivity. However, the uncertainty of effective mass-squared difference $\Delta m_{\mu\mu}^2$ (combination of Δm_{31}^2 and Δm_{32}^2) has large impact to the sensitivity. $\chi^2 \approx 19$ will be achieved by using a 1% uncertainty of $\Delta m_{\mu\mu}^2$ from a prior measurement, shown in Figure 3.

3. Other physics goals

Another important goal of JUNO is precision measurement of mixing parameters. Three mixing parameters, Δm_{21}^2 , Δm_{31}^2 and $\sin^2 \theta_{12}$ can be measured with a precision better than 1% by precisely measuring the reactor antineutrino oscillation spectrum. It will contribute to the unitarity test of PMNS matrix.

Additionally, JUNO can detect more than 4000 IBD reactions assuming a typical supernova burst at the galaxy center. The energy spectrum of electron antineutrinos ($\bar{\nu}_e$) from supernova can be precisely measured. Comparing with water Cerenkov detector, JUNO has smaller energy threshold (below 1 MeV) and thus can also detect hundreds of neutrino scattering events on

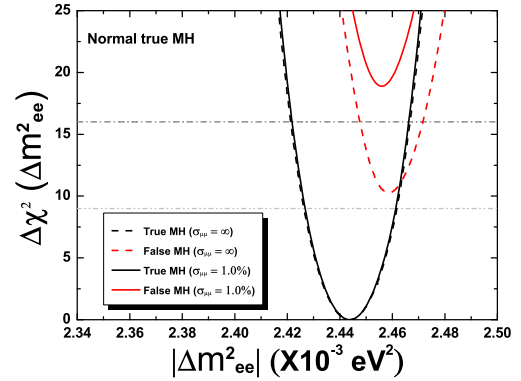


Figure 3: Mass hierarchy sensitivity of JUNO. The vertical difference of the curves for the true and false MHs is χ^2 . The solid and dashed lines are for the analyses with and without the prior measurement of $\Delta m_{\mu\mu}^2$.

protons, $\nu + p \rightarrow \nu + p$. Thus, spectrum information for other neutrino flavors than $\bar{\nu}_e$ can be probed.

Other important goals include observation of geoneutrinos, solar neutrinos and atmospheric neutrinos, and so on.

4. Detector design concepts

As a preliminary design, JUNO detector includes a central detector to detect reactor antineutrinos and a veto detector to reject cosmic muons and induced backgrounds. Figure 4 is the default design option for center detector. The inner 35 m diameter acrylic vessel contains 20 kton liquid scintillator as target to detect reactor antineutrinos. The outer 40 m diameter stainless steel structure holds ~ 17000 20 inch PMTs to collect the scintillation and Cerenkov lights produced by the interactions of antineutrinos in the liquid scintillator. The acrylic vessel and the stainless steel structure are immersed in a water pool. The water pool is filled with purified water and instrumented with PMTs to function as Cerenkov detector to veto the cosmogenic backgrounds. Above the water pool, a muon tracking detectors probably made by plastic scintillator functions as another veto detector to reject cosmogenic backgrounds.

A backup option is also under R&D. The inner vessel is a balloon filled by liquid scintillator and supported by acrylic plates. An outer stainless steel vessel contains mineral oil as shielding and buffer. PMTs are mounted inside of the stainless steel vessel, which is immersed

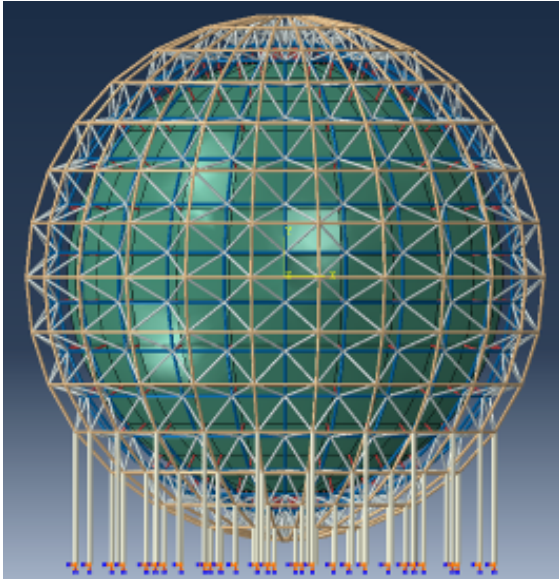


Figure 4: A conceptual design for the center detector.

in the water pool. The energy resolution, radioactivity level and the technical challenges are main concerns for the detector R&D.

5. Technical challenges

One key requirement for JUNO detector is the $3\%/\sqrt{E_{vis}}$ energy resolution which is dominated by the photoelectron (PE) yield, namely the number of PEs collected by the PMTs per 1 MeV visible energy (E_{vis}) produced by the antineutrino interactions in liquid scintillator. To achieve $3\%/\sqrt{E_{vis}}$ energy resolution, an unprecedented PE yield of 1100 PEs/MeV is required. The PE yield can be modeled as $\epsilon \cdot C \cdot Y \cdot e^{-d/L}$, where ϵ is the quantum efficiency (QE) and collection efficiency of converting one optical photon to one PE for PMT, C is the PMT coverage, Y is the scintillation light yield, L is the light attenuation length of the scintillator, d is the transportation distance of the scintillation light. For a large 20 kton detector, better performance of liquid scintillator and PMTs are important to achieve better energy resolution.

For the default design as shown in Figure 4, the PMT coverage can reach to 75-80% by careful arrangement of PMT spacing by minimizing the clearance. R&D efforts are in progress to achieve better performance of liquid scintillator and PMT. The attenuation length of liquid scintillator can be improved from 15 m to 20 m by improving raw material, production process and pu-

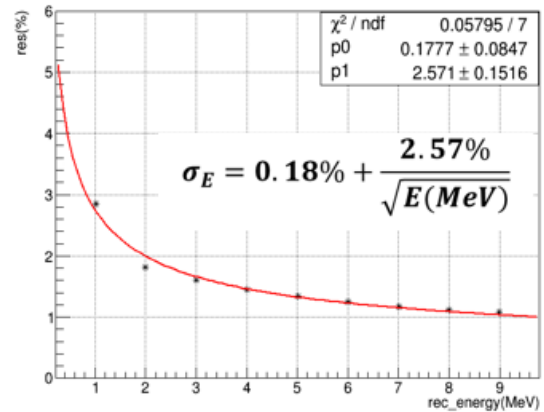


Figure 5: Energy resolution by simulation data using a total charge-based energy reconstruction with an ideal vertex reconstruction.

rification by water extraction, filtration and distillation. A new type of PMT, namely MCP-PMT, can enhance the efficiency by 50-100% compared with the traditional PMT. The high QE PMT using SBA photocathode (such as Hammamatsu R5912-100) with a 35% QE is an alternative option.

The $3\%/\sqrt{E_{vis}}$ energy resolution is possible to achieve, as demonstrated by a Geant4 detector simulation. Figure 5 shows the result using a setup of 77% coverage, 35% QE, and 20 m attenuation length in the simulation software, which has been tuned based on Daya Bay experiment data.

6. Summary

JUNO experiment is aimed at neutrino mass hierarchy determination. Using a 20 kton liquid detector with a $3\%/\sqrt{E_{vis}}$ energy resolution, the sensitivity is $3\sigma-4\sigma$ by 6 year running. Additionally, three mixing parameters can be measured with a precision better than 1%. Other rich physics goals include observation of supernova neutrinos, geo-neutrinos, solar neutrinos, and atmospheric neutrinos. The physics potential is strong, meanwhile the technical challenges are significant. The JUNO project was approved by Chinese Academy of Sciences in 2013 and is planned to be in operation in 2020.

References

- [1] F. P. An *et al.* [DAYA-BAY Collaboration], Phys. Rev. Lett. **108**, 171803 (2012).
- [2] Y. Abe *et al.* [DOUBLE-CHOOZ Collaboration], Phys. Rev. Lett. **108**, 131801 (2012).

- [3] J. K. Ahn *et al.* [RENO Collaboration], Phys. Rev. Lett. **108**, 191802 (2012).
- [4] F. P. An *et al.* [Daya Bay Collaboration], Chin. Phys. C **37** (2013) 011001
- [5] F. P. An *et al.* [Daya Bay Collaboration], Phys. Rev. Lett. **112** (2014) 061801
- [6] K. Abe *et al.* [T2K Collaboration], Phys. Rev. Lett. **107**, 041801 (2011).
- [7] P. Adamson *et al.* [MINOS Collaboration], Phys. Rev. Lett. **107**, 181802 (2011).
- [8] A. Samanta, Phys. Lett. B **673**, 37 (2009).
- [9] D. J. Koskinen, Mod. Phys. Lett. A **26**, 2899 (2011).
- [10] HyperK Collaboration, (K. Abe *et al.*), arXiv:1109.3262.
- [11] LBNE Collaboration, (T. Akiri *et al.*), arXiv:1110.6249.
- [12] S. Bertolucci *et al.*, arXiv:1208.0512.
- [13] S. T. Petcov and M. Piai, Phys. Lett. B **533**, 94 (2002).
- [14] S. Choubey, S. T. Petcov and M. Piai, Phys. Rev. D **68**, 113006 (2003).
- [15] J. Learned, S. T. Dye, S. Pakvasa and R. C. Svoboda, Phys. Rev. D **78**, 071302 (2008).
- [16] L. Zhan, Y. Wang, J. Cao and L. Wen, Phys. Rev. D **78**, 111103 (2008).
- [17] L. Zhan, Y. Wang, J. Cao and L. Wen, Phys. Rev. D **79**, 073007 (2009).
- [18] Y.F. Li, J. Cao, Y. Wang and L. Zhan, Phys.Rev. D **88**, 013008 (2013).
- [19] M. Blennow, P. Coloma, P. Huber and T. Schwetz, JHEP **1403** (2014) 028